HYDROLOGICAL PROCESSES
Hydrol. Process. **20**, 469–486 (2006)
Published online 18 October 2005 in Wiley InterScience (www.interscience.wiley.com). DOI: 10.1002/hyp.5915

A simulation model for unified interrill erosion and rill erosion on hillslopes

Q. Q. Liu,[1]* H. Xiang[1] and V. P. Singh[2]

[1] *Institute of Mechanics, Chinese Academy of Sciences, Beijing 100080, People's Republic of China*
[2] *Department of Civil and Environmental Engineering, Louisiana State University, Baton Rouge, LA 70803-6405, USA*

Abstract:

A mathematical model was developed for simulating runoff generation and soil erosion on hillslopes. The model is comprised of three modules: one for overland flow, one for soil infiltration, and one for soil erosion including rill erosion and interrill erosion. Rainfall and slope characteristics affecting soil erosion on hillslopes were analysed. The model results show that the slope length and gradient, time distribution rainfall, and distribution of rills have varying influence on soil erosion. Erosion rate increases nonlinearly with increase in the slope length; a long slope length leads to more serious erosion. The effect of the slope gradient on soil erosion can be both positive and negative. Thus, there exists a critical slope gradient for soil erosion, which is about 45° for the rate of erosion at the end of the slope and about 25° for the accumulated erosion. Copyright © 2005 John Wiley & Sons, Ltd.

KEY WORDS erosion characteristics; hillslope; interrill erosion; overland flow; soil erosion model; rill erosion; soil infiltration

INTRODUCTION

On a hillslope, overland flow first generates sheet erosion (interrill erosion) and then with increasing flux it causes rill erosion. Interrill erosion and rill erosion are two basic types of soil erosion on rural and agricultural watersheds. When a rainstorm occurs, both are commonly observed to coexist on steep slopes, especially in the Loess Plateau area of China. Therefore, a soil erosion model, in general, ought to include these two parts, i.e. interrill erosion and rill erosion. Owing to their different flow and erosion characteristics, both are commonly investigated separately.

Interrill erosion and rill erosion have been extensively investigated for over half century. Many empirical and semi-empirical relationships have been derived for determining the rate of interrill erosion (Liebenow *et al.*, 1990; Grosh and Jarrett, 1994; Sharma *et al.*, 1995; Bradford and Foster, 1996; Zhang XC *et al.*, 1998; Bulygin, 2001). Likewise, a multitude of empirical and theoretical models of rill erosion have been developed (Moore and Burch, 1986; Elliot and Laflen, 1993; Tang and Chen, 1997; Zhang KL *et al.*, 1998; Li *et al.*, 2003).

The universal soil loss equation (USLE; Wischmeier and Smith, 1965, 1978) and the revised USLE (RUSLE; Renard *et al.*, 1991) have been popular empirical models and have been extensively applied throughout the world to predict soil erosion from agricultural, forest, and urban areas. However, since soil and rainfall characteristics substantially vary in different regions, these empirical models do not reflect the overall effect of various factors affecting soil erosion. These are lumped models and do not have the ability to describe the spatial variability of soil erosion in a watershed, which may be needed in solute transport modelling and environmental impact assessment. This is partly the reason that these days

* Correspondence to: Q. Q. Liu, Department of Civil and Environmental Engineering, Baton Rouge, LA 70803-6405, USA.
E-mail: cesing@lsu.edu

Received 24 February 2004
Accepted 18 January 2005

there seems to be a shift in emphasis from empirical modelling to process-based dynamic modelling. As a result, a number of process-oriented dynamic models of soil erosion have been developed. Examples of such models are the Water Erosion Prediction Project (WEPP) model (Foster *et al*., 1989; Ascough *et al*., 1997), the areal nonpoints source watershed environment response simulation (ANSWERS) model (Beasley *et al*., 1980), the agricultural nonpoint source (AGNPS) model (Young *et al*., 1989; Perrone and Madramootoo, 1999), the kinematic erosion simulation (KINEROS) model (Woolhiser *et al*., 1990), and the Limburg soil erosion model (LISEM; De Roo *et al*., 1996), among others. On the other hand, some soil erosion prediction models are stochastic (Lisle *et al*., 1998) or are based on artificial neural networks (Gautam *et al*. 2000). More recently, two-dimensional overland flow and erosion models have also been developed (Singh *et al*., 2001; Tayfur, 2001, Liu *et al*., 2004). The WEPP model, among others, is a typical example that combines rill erosion with interrill erosion and builds a steady sediment transport equation.

One of the reasons for developing physically based models has been to improve prediction of soil erosion. However, because of the complexity of soil erosion, fully physically based models have not yet become a practical tool. Most such models employ the concept of steady-state sediment transport, although the actual soil erosion and transport process is unsteady. Investigations that have incorporated unsteady dynamics of soil erosion have been relatively few. Furthermore, most of the models have been applied to predict soil erosion from a watershed, and do not discuss the characteristics of erosion on a hillslope. This may partly be due to inadequate knowledge of physical and chemical processes leading to soil erosion and the paucity of experimental and field data. Therefore, the objective of this study was to develop a dynamic soil erosion model based on physical processes and investigate the characteristics of soil erosion including rill erosion and interrill erosion on hillslopes.

PROPOSED SOIL EROSION MODEL

Soil erosion on hillslopes is a complex process that entails the processes of overland flow, infiltration, and erosion. Thus, the model includes three component models: a soil infiltration model, a surface flow model, and a soil erosion model.

Soil infiltration

The overland flow model requires an infiltration component to produce rainfall excess which can then be routed down the hillslope. A revised Green–Ampt infiltration model was employed to describe the process of rainfall infiltration. Mein and Larson (1973) extended the classical Green–Ampt formulation for application to cases with constant rainfall rate p producing ponding conditions at times $t > 0$.

When the infiltration rate i equals the rainfall rate p, assumed as constant, the cumulative infiltration I_p is expressed as

$$I_p = \frac{(\theta_\mathrm{s} - \theta_\mathrm{i})S}{p/K - 1} \tag{1}$$

where K (m s^{-1}) is the saturated hydraulic conductivity of the soil, θ_s (m^3 m^{-3}) is the saturated volumetric water content, i.e. the effective porosity θ_i (m^3 m^{-3}) is the initial volumetric water content, and S (m) is the soil suction. The time to ponding t_p (s) is obtained from Equation (1) as

$$t_\mathrm{p} = I_\mathrm{p}/p \tag{2}$$

Thus, the infiltration rate during the whole overland flow process can be expressed as a function of cumulative infiltration I in the form

$$\begin{aligned} i &= p, & t &\le t_\mathrm{p} \\ i &= K[1 + (\theta_\mathrm{s} - \theta_\mathrm{i})S/I], & t &> t_\mathrm{p} \end{aligned} \tag{3}$$

In order to express infiltration as a function of time, Equation (3) is rewritten as

$$K(t - t_p) = I - I_p - S(\theta_s - \theta_i)\ln\left[\frac{I + S(\theta_s - \theta_i)}{I_p + S(\theta_s - \theta_i)}\right] \tag{4}$$

However, steady rainfall is seldom observed in nature. A generalized version of the Mein–Larson model was proposed by Chu (1978), generalized as the GA-ML model for unsteady rainfall. For each time step the generalization characterized the ground surface status into four situations: (1) no ponding at the beginning, no ponding at the end; (2) no ponding at the beginning, ponding at the end; (3) ponding at the beginning, no ponding at the end; and (4) ponding at the beginning, ponding at the end.

Overland flow

The depth of overland flow generally is very small and its boundary conditions are complex. Therefore, it is difficult to apply the whole St Venant equations for modelling it. The kinematic wave approximation (Lighthill and Witham, 1955) to the St Venant equations has long been applied successfully to hillslopes (Woolhiser and Liggett, 1967; Woolhiser, 1975; Cundy and Tento, 1985; Singh, 1996, 1997). Using the assumption that the gravitational force along the slope is equal to the resistance force, a concise relationship between discharge and water depth can be established based on the Manning equation. Under the assumption that rainfall occurs vertically, Chen and Liu (2001) found that the steep hillslope gradient for receiving rainfall was significant on the Loess Plateau of China; therefore, the rainfall intensity for steep slope surfaces need to be modified as $p\cos\theta$ (p is the actual rainfall intensity and θ is the inclination angle of the slope). The governing equations of overland flow on the steep hillslopes can be written as:

$$\frac{\partial h}{\partial t} + \frac{\partial q}{\partial x} = p\cos\theta - i \tag{5}$$

$$q = \frac{1}{n}h^{5/3}S_0^{1/2} \tag{6}$$

where x (m) is the distance down slope, h (m) is the water depth, q (m^2 s^{-1}) is the unit width discharge, θ is the inclination angle of slope (degrees), n (s m$^{-1/3}$) is the Manning roughness coefficient, and S_0 is the slope gradient ($S_0 = \sin\theta$).

For hillslopes, the surface flow equations described by Equations (5) and (6) can be assumed to have the following initial and boundary conditions:

$$\begin{aligned} q(0, t) &= 0, \quad t \geq 0 \\ q(x, 0) &= 0, \quad x \geq 0 \end{aligned} \tag{7}$$

Soil erosion

Soil erosion depends on the generation of overland flow. It is assumed that the influence of soil erosion on overland flow is negligible. This permits determination of runoff and soil infiltration independently and then soil erosion. Soil erosion on hillslopes can be divided into interrill erosion and rill erosion, which can be described by the following sediment continuity equation (Xiang, 2002):

$$\frac{\partial hC}{\partial t} + \frac{\partial qC}{\partial x} = D_r + D_i \tag{8}$$

where C (kg m^{-3}) is the sediment concentration, D_r (kg s^{-1} m^{-2}) is the rill erosion rate, and D_i (kg s^{-1} m^{-2}) is the interrill erosion rate. Interrill erosion D_i in the model represents the process of sediment detachment and delivery to rills.

Interrill erosion. Interrill erosion depends on soil and slope characteristics, vegetation and land use, rainfall intensity, and hydraulic factors of runoff (Bradford and Foster, 1996), and reflects the capacity of thin, shallow flow to transport and disperse soil on the hillslope. Raindrop impact detaches soil particles and splash causes soil transport, soil characteristics determine the erosion-resistance of the soil, and the soil detachment is the source of interrill erosion. Interrill flow not only transports soil particles, but also detaches soil particles. Based on experiments conducted on a soil flume with artificial rainfall at the Northwestern Institute of Water and Soil Conservation, Chinese Academy of Science, a formula for interrill erosion rate by using the grey relation analysis and regression analysis (Xiang, 2002) was derived:

$$\frac{D_i d}{R_c} = 1{\cdot}8 \times 10^{-9} \left(\frac{h}{d}\right)^{1{\cdot}5} (1{\cdot}05 - 0{\cdot}85 e^{-4 \sin\theta}) \tag{9}$$

where R_c (kg s^{-1} m^{-1}) is the saturated sediment-transport capacity of interrill flow, and d (m) is the diameter of soil particles.

The saturated sediment-transport capacity of interrill flow R_c can be calculated by using the following formula due to Low (1989):

$$R_c = \frac{6{\cdot}42}{(s-1)^{0{\cdot}5}} (Y - Y_c) d\, S_f^{0{\cdot}6} u \rho_s \tag{10}$$

where Y is the dimensionless shear stress, $Y = \tau/[(\rho_s - \rho)gd]$; Y_c is the dimensionless critical shear stress, $Y_c = \tau_c/[(\rho_s - \rho)gd]$; τ (Pa) is the flow shear stress; τ_c (Pa) is the critical shear stress, which can be obtained from Govers' (1987) investigation; ρ (kg m^{-3}) is the density of fluid; ρ_s (kg m^{-3}) is the density of sediment; $s = \rho_s/\rho$; g (m s^{-2}) is the gravitational acceleration; S_f is the energy slope; and u (m s^{-1}) is the mean velocity of runoff.

Rill erosion. Using a series of small-scale erosion experiments in laboratory, a rill erosion model was developed by Li *et al.* (2003). This model employed the same concepts of sediment transport as used in open channels. Assuming that the rill erosion rate is proportional to the difference between the maximum sediment transport capacity of rill flow T_c (kg s^{-1} m^{-1}) and the actual sediment transport rate q_s (kg s^{-1} m^{-1}), one has

$$D_r = \alpha(T_c - q_s) \tag{11}$$

where α (m^{-1}) is a coefficient and its reciprocal, $1/\alpha$, with a length dimension, denotes the distance that the sediment concentration of rill flow re-establishes from zero to the maximum capacity. This means that the erosion capacity of flow has a limited value which does not exceed αT_c. If the hydraulic condition of flow remains unchanged, then the erosion capacity of flow will gradually decrease with increasing sediment concentration of flow until it reaches its maximum value.

Considering the influence of various factors, such as the effective shear stress of the rill flow, the hydraulic radius, the flow velocity, the diameter of soil particles, the density of soil particles under water, and the slope gradient, by dimensional analysis and multiple regression analysis of experimental data we obtained the following relationship (Li *et al.*, 2003):

$$\frac{1/\alpha}{R} = 1{\cdot}5 \times 10^4 \left[\frac{\tau - \tau_c}{(\rho_s - \rho)gd}\right]^{0{\cdot}15} \left(\frac{u}{\sqrt{gd}}\right)^{-1} S_0^{1{\cdot}5} \tag{12}$$

where R (m) is the hydraulic radius, τ (Pa) is the flow shear stress, τ_c (Pa) is the critical shear stress, and S_0 is the slope gradient ($S_0 = \sin\theta$).

The sediment transport rate of rill flow can be calculated by Yalin's formula (Yalin, 1963):

$$T_c = GY^{0\cdot5}(Y - Y_c)d[gd(s-1)]^{0\cdot5}\rho_s \tag{13}$$

$$G = \frac{0\cdot635}{Y_c}\left[1 - \frac{\ln(1+\mathrm{as})}{\mathrm{as}}\right] \tag{14}$$

$$\mathrm{as} = \frac{2\cdot45}{s^{0\cdot4}}Y_c^{0\cdot5}\left(\frac{Y}{Y_c} - 1\right) \tag{15}$$

In general, the process of erosion in rill flow is similar to the process of sediment transport in open channel flow. Dou's (1999) formula was chosen for describing the critical shear stress τ_c. The formula expresses the law of incipient motion of sediments of various diameters, such as coarse sediment, fine sediment, cohesive sediment, and light sediment. For fine sediments like soil, this formula considers two components of the cohesive force between particles and the additional pressure of water film. In addition, slopes on the Loess Plateau are usually large, so the influence of slope on a soil particle's incipient motion should be taken into account. On a slope, it can be expressed as

$$\tau_c = k^2\rho\left(\frac{d'}{d_*}\right)^{1/3}\left[3\cdot6\left(\frac{\rho_s - \rho}{\rho}\right)gd\ \cos\theta + \left(\frac{\gamma_0}{\gamma_{0^*}}\right)^{5/2}\left(\frac{\varepsilon_0 + g\ \cos\theta h\delta\sqrt{\delta/d}}{d}\right)\right] \tag{16}$$

where k is a nondimensional parameter, $k = 0\cdot128$; d' (m) is the characteristic diameter ($d' = 0\cdot5$ mm, $d \le 0\cdot5$ mm, $d' = d$, $0\cdot5 < d < 10$ mm); d_* (m) is the reference diameter, taken as 10 mm; ε_0 (m^3 s^{-2}) is the parameter of the adhesion force, for ordinary sediments $\varepsilon_0 = 1\cdot75$ cm^3 s^{-2}; δ (m) is the thickness parameter of the water film, $\delta = 2\cdot31 \times 10^{-5}$ cm; γ_0 (N m^{-3}) is the dry specific weight of soil; and γ_{0^*} (N m^{-3}) is the stable dry specific weight of soil.

ANALYSIS OF UNSTEADY SEDIMENT TRANSPORT EQUATION

Using $q = uh$, $q_s = qC$ and the flow continuity equation, Equation (8) may be transformed to the following form:

$$\frac{\partial C}{\partial t} + u\frac{\partial C}{\partial x} = S_r(C) \tag{17}$$

Here, $S_r(C) = (1/h)[\alpha(T_c - qC) + D_i - C(p\cos\theta - i)]$ and the following initial and boundary conditions were employed:

$$C(0,\ t) = 0, \quad t \ge 0$$
$$C(x,\ 0) = 0, \quad x \ge 0 \tag{18}$$

Equation (17) for the unsteady sediment transport equation is a hyperbolic-type equation with initial and boundary value problem expressed by Equation (18). Expressing the source term $S_r(C)$ as $S_r = -ac + b$, Equation (17) becomes

$$\frac{\partial C}{\partial t} + u\frac{\partial C}{\partial x} = -aC + b \tag{19}$$

Here, $a(x,\ t) = (1/h)(\alpha q + p\cos\theta - i)$, $b(x,\ t) = (1/h)(\alpha T_c + D_i)$, and $u = u(x, t)$ is the velocity of overland flow that was assumed not to be associated with sediment concentration C.

At any point of time, the distribution of u is assumed as a progressively increasing function with x. This shows that the solution cannot experience interruption. If large obstacles exist along the direction of runoff, which may lead to u decreasing with x, then it will be possible to experience interruption.

When overland flow reaches a steady state, a and b can be approximated as constants. Equation (19) can be written in the following characteristic form:

$$\frac{dC}{dt} = -aC + b \tag{20}$$

$$\frac{dx}{dt} = u(x,\ t) \tag{21}$$

with the initial condition: $C(x, 0) = 0$. Thus, Equation (20) has the following solution:

$$C = \frac{b}{a}(1 - e^{at}), \text{ along curve}: \frac{dx}{dt} = u(x,\ t) \tag{22}$$

If $a < 0$, then C becomes negative and the solution will be physically unrealistic. Therefore, the accuracy of the α value is very important. When $t \to \infty$, that is $C \to b/a$, the sediment concentration depends on $(\alpha T_c + D_i)/(\alpha q + p\cos\theta - i)$. This shows that sediment concentration depends on rainfall intensity, hydraulic characteristics of overland flow, and soil characteristics. In addition, one can use $C \to b/a$ to examine numerical results and judge the adequacy of the numerical method.

The unsteady sediment transport Equation (17) is a hyperbolic differential equation with source term. For solving the equation accurately, the space–time conservation element and solution element method, or the CE/SE method for short, originally proposed by Chang (1995; Chang *et al.*, 1999) was employed to solve the unsteady sediment conservation equation numerically. The CE/SE method is a novel numerical framework for conservation laws and is different from some traditional numerical methods in many features. Through a unified treatment of space and time, and the introduction of a conservation element and solution element, the numerical framework can strictly assure the conservation laws for any physical quantity.

MODEL VALIDATION

The data set for verification of the model was obtained from experiments conducted on a soil flume with artificial rainfall at the Northwestern Institute of Water and Soil Conservation, Chinese Academy of Science, China. The test plot was a 3·2 m long, 1·0 m wide, and 0·3 m deep wooden box with holes at the bottom. The slope or the gradient of the test plot was adjustable and was varied. The soil used in the experiment was the local loess with a median grain size of sediment $d_{50} = 0{\cdot}02$ mm. The soil was packed to a 25 cm thickness with a plane surface in the wooden box. Rainfall was simulated by a drop-former-type rainfall simulator of artificial precipitation in which raindrops were formed at 16 m above from the surface of the test plot and the falling raindrops attained a fixed speed near the surface. The rainfall intensity was adjusted in the range of 15–200 mm h^{-1}. Before and after the experiment, the bulk density, moisture content and porosity of the soil were measured using a ring sampler. The bulk density of the soil was 1·33 g cm^{-3}, the initial moisture content of soil $\theta_i = 0{\cdot}2206$ and the porosity of the soil, i.e. the saturated volumetric water content, was $\theta_s = 0{\cdot}5027$. According to Jiang (1997), the infiltration coefficient K and the suction S of loess soil used in experiments are $1{\cdot}67 \times 10^{-6}$ m s^{-1} and 0·15 m respectively.

The runoff discharge, runoff volume, and sediment concentration were measured at the outlet of the test plot for different rainfall intensities and slopes (gradients). To determine the runoff discharge and sediment concentration, runoff samples containing the sediment were collected at the outlet of the test plot. Samples of approximately 300 ml were obtained using beakers. The flow discharges were obtained by dividing the sample volume by the collection time, and the sediment concentrations in each of these samples were determined later by weighing on scales after baking. At the same time, all of the runoff at the outlet was collected, which was continuously measured in a cylindrical container to determine the runoff volume. Then, the accumulated erosion quantity was determined from the measurements of runoff discharge, sediment concentration, and runoff volume as well. In addition, the mean flow velocities of several specific points were also measured using the stained method at different times from the beginning of runoff formation.

Two sets of experimental data were used to verify the model proposed in this paper. In one experiment (Case A), the rainfall intensity was 2·06 mm min^{-1}, the inclination angle of the slope was 15°, and the rill erosion began to generate at 3 min 20 s. In the other experiment (Case B), the rainfall intensity was 1·34 mm min^{-1}, the inclination angle of the slope was 20°, and the rill erosion began to generate at 35 min. Comparisons of the two cases of observed values and the values predicted by the proposed model at the outlet are shown in Figures 1 and 2. Overall, good agreements were found between observed and predicted values of discharge hydrographs, mean runoff velocities, sediment concentrations, and accumulated erosion amounts. In addition, the results shown in Figure 2 show that, when rills occurred on the slope, the quantity of soil eroded increased rapidly.

Owing to the lack of field observations, we only validated the model using laboratory experiments. Nevertheless, the results indicate that the model comprising a kinematic wave model and an unsteady erosion model is capable of adequately simulating the process of runoff generation and soil erosion on steep loess hillslopes. The model has potential for predicting soil erosion on the Loess Plateau of Northwest China.

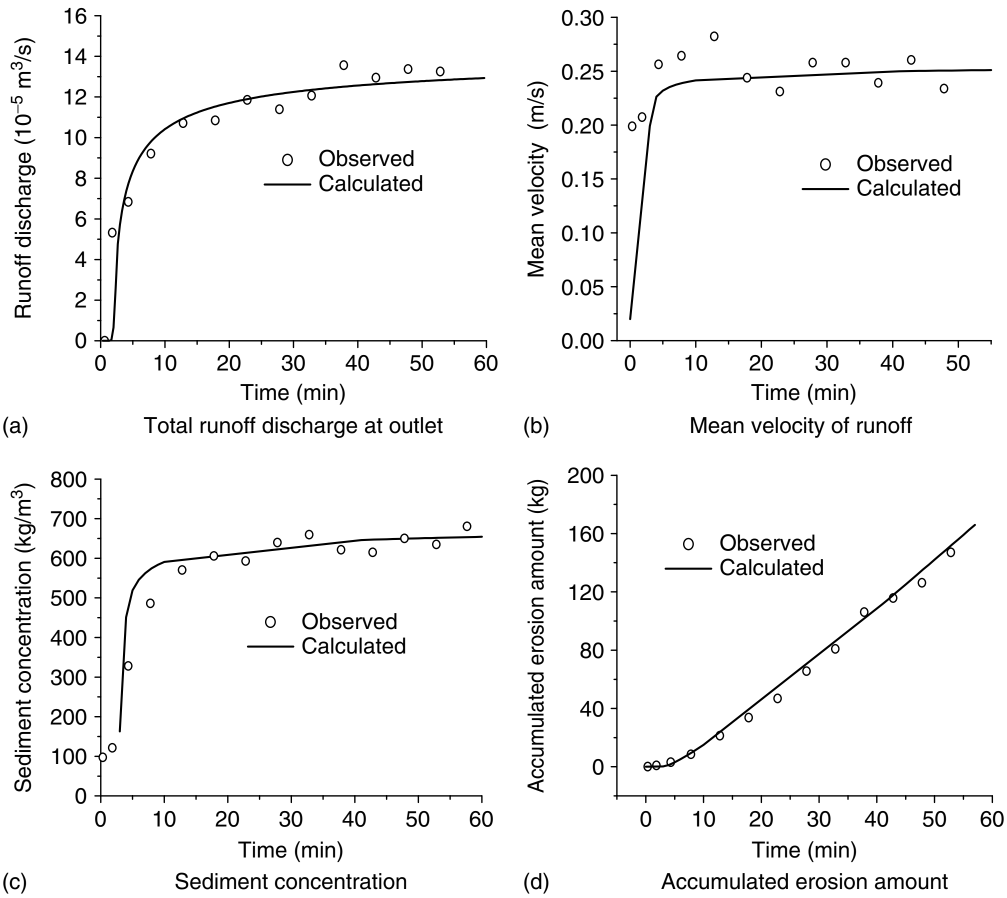

Figure 1. Comparison of experimental and predicted results (rainfall intensity: 2·06 mm min^{-1}; inclination angle of slope: 15°; time in which rill occurs: 3 min 20 s)

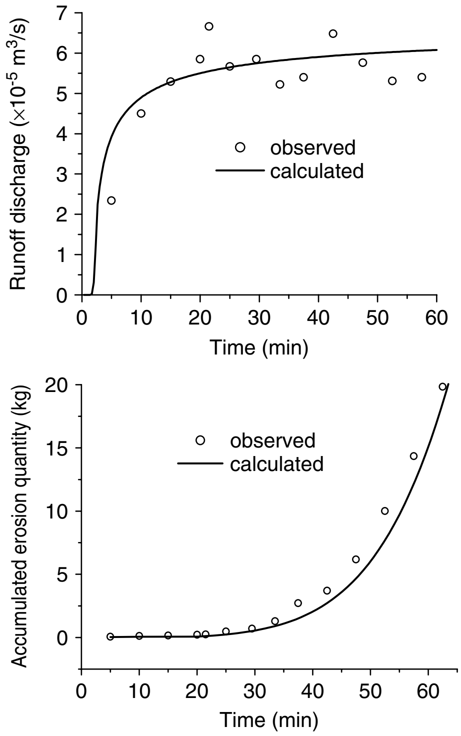

Figure 2. Comparison of experimental and predicted results (rainfall intensity: 1·34 mm min^{-1}; inclination angle of slope: 20°; time in which rill occurs: 35 min)

SOIL EROSION CHARACTERISTICS ON SLOPES

The Loess Plateau area of China is a semi-humid and semi-arid region. Serious soil erosion over long periods leads to extremely complex fragmentation of surface morphology. The lengths and slope gradients of existing hillslopes differ appreciably. Commonly, the length of a hillslope may vary from several metres to nearly several hundred metres, and the slope gradient of hillslopes can vary from 2° to 60°. In addition, the seasonal distribution of precipitation is highly nonuniform, and the rainfall intensity of rainstorms is also quite different. Most rainstorms are of short duration and indefinite location (Wang and Jiao, 1996; Jiang, 1997). These extreme differences in topography and rainfall lead to different characteristics of soil erosion on the Loess Plateau. Therefore, the study of the basic characteristics of soil erosion on slopes is essential for the protection of soil in the Loess Plateau area.

The influences of the length and slope gradient of hillslopes, rainfall intensity and distribution, and the distribution of rill density were analysed by applying the proposed soil erosion. The soil characteristics were assumed to be relatively homogeneous. The method of Yang (1996) and Jiang (1997) was used to determine the characteristic parameters of loess soil and other parameters used in calculation, and these parameters are shown in Table I, where L is the slope length, W is the width of slope, D is the spacing interval between two rills, and c_f is the conflux coefficient of overland flow concentrating into rills. In the model, c_f is used to calculate the discharge of rill flow. For example, the conflux coefficient of rill flow was taken as 0·8, namely 80% of overland flow in interrill areas concentrated into rills. Other symbols are as defined before.

Influence of rainfall intensity

Taking the soil parameters from Table I, soil erosion on the slope was simulated for six rainfall intensities of 0·5, 1·0, 1·5, 2·0, 2·5, and 3·0 mm min^{-1}. The calculated values of unit sediment transport rate and unit

Table I. Characteristic parameters used in calculation

θ_s (m^3 m^{-1})	57
θ_i (m^3 m^{-1})	12
K (mm h^{-1})	0·75
S (m)	0·06
d (mm)	0·05
γ_0 (N m^{-3})	1300
γ_{0*} (N m^{-3})	1100
W (m)	5
L (m)	30
S_0	sin(30°)
p (mm min^{-1})	1
D (m)	0·50
c_f	0·8

accumulated erosion amount as functions of time for various rainfall intensities are shown in Figure 3a and b respectively. The simulated results show that both the unit sediment transport rate and the unit cumulative erosion amount increased remarkably as the rainfall intensity increased. This is easy to understand, because increased rainfall intensity directly leads to increased discharge, which results in increased eroding capability and the attendant increased erosion. However, it is worth noting that both the unit sediment transport rate and the unit accumulated erosion amount do not increase linearly with rainfall intensity. There are two reasons for this. First, the excess rainfall increases more for rainstorms with greater rainfall intensity; second, the eroding and transport capability of runoff does not increase linearly with runoff. The result is that large rainstorms easily cause greater erosion. Indeed, what is unique about erosion on the Loess Plateau is that the bulk of it always occurs during large rainstorms. On average, three rainfall events occupying only about 4% of the total rainfall in each year may cause serious erosion (Wang and Jiao, 1996). That is why the erosion of the Loess Plateau under rainstorm conditions is emphasized here.

Figure 3c shows the unit sediment transport rate varying along the slope for various rainfall intensities. The results show that the rate of erosion increases more and more quickly along the slope. This indicates that soil erosion increases with the increase of the slope length. This will be discussed in more detail later.

Influence of rainfall pattern

Rainfall events are often nonuniform and their varying intensity has a significant effect on soil erosion on slopes. To analyse the influence of rainfall, rainstorms of types A and B with the same rainfall amount were chosen. The peak of the type A rainstorm is at the beginning of the duration, and the peak of type B is toward the end, as shown in Figure 4.

Keeping other parameters unchanged (see Table I), soil erosion was calculated for these two kinds of rainstorm (types A and B). Figure 5 illustrates the simulation results of unit discharge, mean velocity, unit sediment transport rate, and unit accumulated erosion amount as functions of time. Figure 5a and b shows little difference between rainfall type A and rainfall type B. Although the differences between them are small, the comparison nevertheless shows that the flow discharge and mean velocity peaks for rainfall type B are a little greater than those for rainfall type A. These results demonstrate the trend that the later the rainfall peak value, the higher the maximum value of the main hydraulic parameter. In the initial period of rainfall the infiltration rate is high and then it rapidly starts decreasing; as a result, the infiltration rate becomes lower and steadier and the rainfall excess rate becomes higher with time for the same intensity of rain. This is the reason that the later the rainfall peak, the higher the eroding capability of runoff at the moment of the peak value. This finding was also supported by the calculated unit sediment transport rate and the unit accumulated erosion amount, as shown in Figure 5c and d respectively. The peak of unit sediment transport rate for rainfall type

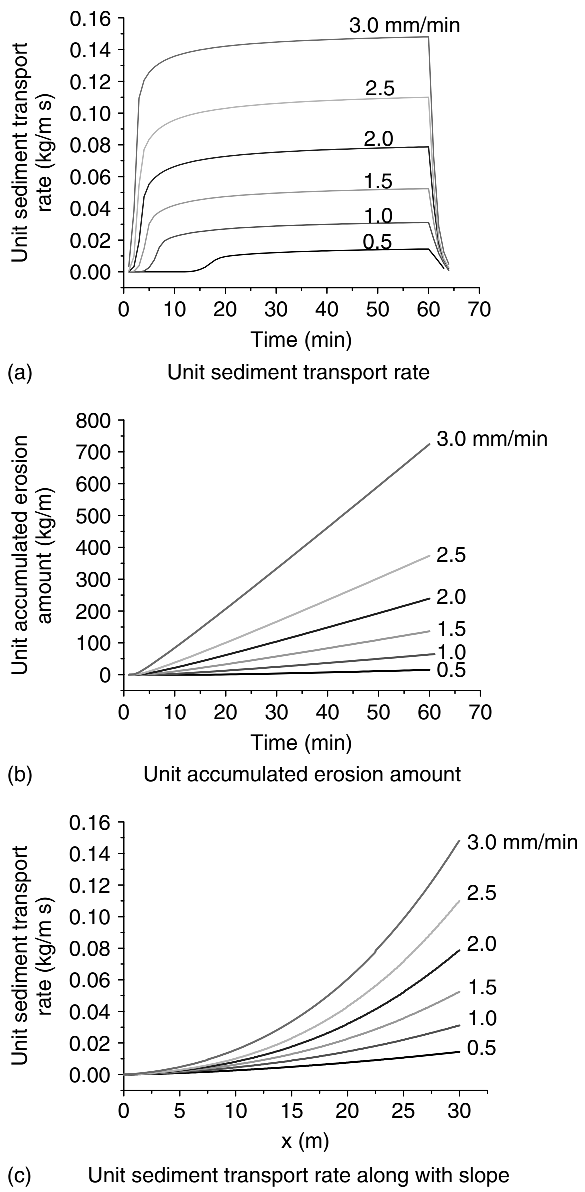

Figure 3. Influence of rainfall intensity on soil erosion

B is a little greater than that for rainfall type A. Similarly, the unit accumulated erosion amount for rainfall type B is a little greater than for rainfall type A. This indicates that the same rainfall quantity but different rainfall process may generate somewhat different erosion values. The later peak value of the rainstorm may lead to more serious soil erosion.

Influence of slope length on soil erosion

Under the condition of uniform rainfall intensity (1 mm $\min^{-1}$), soil erosion was simulated for five slope lengths of 10, 20, 30, 40, and 50 m. Figure 6a and b shows the calculated unit sediment transport rate and unit

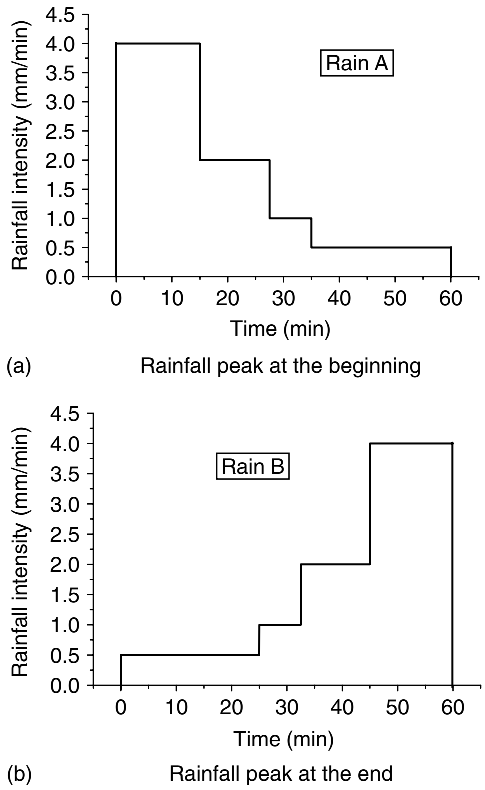

Figure 4. Two types of rainfall

accumulated erosion amount as functions of time for various slope lengths respectively. The calculated results show that both the unit sediment transport rate and unit accumulated erosion amount increased remarkably as the slope length increased. In the initial period of erosion the sediment transport rate of runoff increased quickly, then gradually tended to a steady value. The shorter the slope length was, the faster this process ended. Correspondingly, the accumulated erosion amount increased slowly in the initial period, and then gradually reached a linear increase. In addition, the simulation results illustrated in Figure 2c show that the sediment transport rate increased nonlinearly along the slope, i.e. it did not increase linearly with the slope length. With the increase of the slope length, soil erosion was greater. This indicates that the influence of the slope length became gradually weaker when the slope length decreased to a certain extent. This result reveals that short slopes would be beneficial for decreasing soil erosion. This observation also suggests that cutting and shortening of slope length would be an effective measure for soil erosion protection measures.

Effect of slope gradient on soil erosion

For a uniform rainfall intensity (1 mm min^{-1}), soil erosion was calculated for 15 slope gradients from 5° to 75° in 5° increments. The simulation results are illustrated in Figure 7. The influence of the slope gradient on soil erosion was rather complex. For steady erosion, the calculation results show that the erosion rate at the outlet and accumulated erosion amount initially increased with the slope gradient, and then began to decrease when the slope gradient reached a critical value. However, the corresponding critical slopes for erosion rate at the outlet and accumulated erosion amount were not equal. The erosion rate reached a maximum value at about 45° of the slope gradient, and the maximum value of accumulated erosion amount occurred at about 25° of the slope gradient.

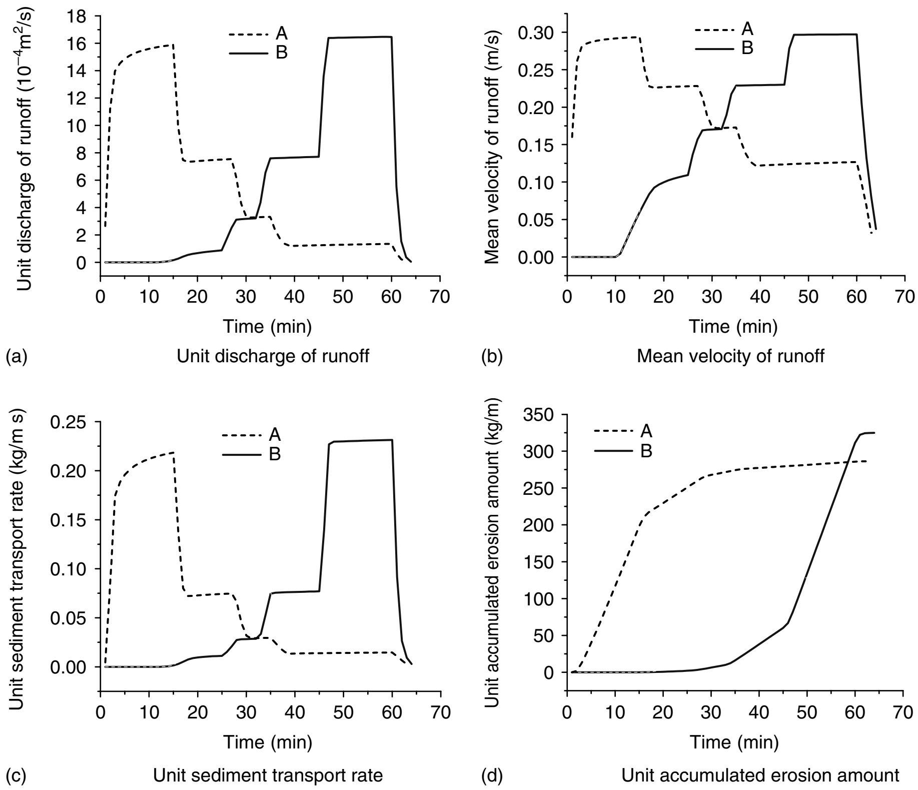

Figure 5. Runoff hydraulic and erosion characteristics for two different rainfall patterns

The influence of slope gradient on runoff generation on hillslopes was also analysed (Liu *et al.*, 2001; Chen *et al.*, 2001; Li *et al.*, 2003). The flow velocity and shear stress at the outlet initially increased with the slope gradient, and then began to decrease when the slope gradient reached a critical value. Although the corresponding critical slopes were not equal, both of them were found within the range of about 40–50°. The erosion rate mainly depends on velocity and shear stress of runoff, so it is easy to understand that erosion rate has a critical slope gradient at about 45°. However, the variation of erosion rate along the slope is nonlinear and is also different for different slope gradients. Thus, the critical value of the accumulated erosion amount occurred at about 25°. This is one of the reasons that most theoretical analysis results give greater critical slopes of about 40–50°, and most experimental observations yield smaller critical slopes of about 20–30°. Most theoretical results were obtained from an analysis of the eroding capability, i.e. erosion rate of overland flow, but most experimental results were obtained by analysing the total erosion quantity, i.e. accumulated erosion amount.

The slope gradient is one of the most important factors affecting the surface flow erosion. The above analysis shows that it is more important to decide the critical slope of soil erosion from accumulated erosion amount. The results obtained here may be significant for programming the utilization of slope land in the Loess Plateau area of China.

Distribution density of rill on soil erosion

On a hillslope, the number and distribution of rills are usually random. However, rill erosion is important for soil erosion on hillslopes. Using the soil erosion model, the influence of the distribution of rills (number of rills in unit width or space interval between two rills) on soil erosion was quantified. Using the parameters

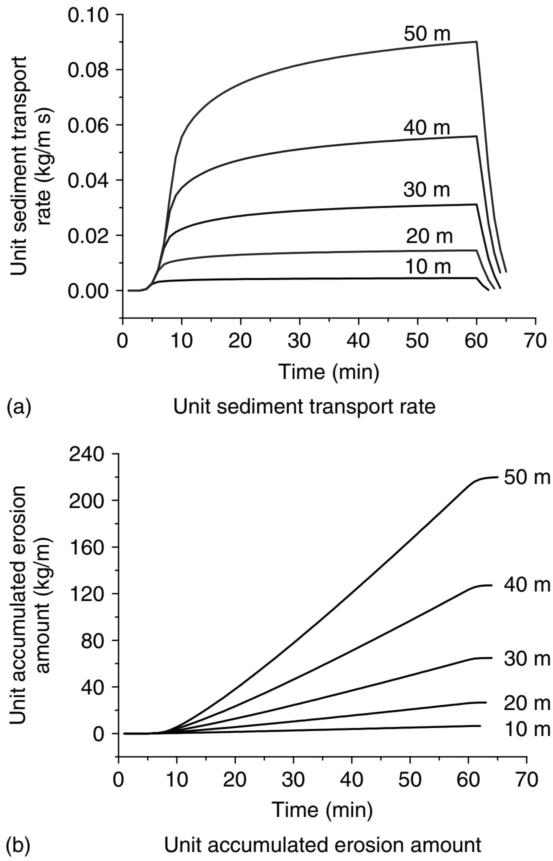

Figure 6. Influence of slope length on soil erosion

given in Table I, soil erosion was calculated for four rill spacing intervals of 0·25, 0·5, 1, and 2 m. The simulation results of unit sediment transport rate and accumulated erosion amount as functions of time are illustrated in Figure 8.

The results show that the sediment transport rate and accumulated erosion amount are different for the four different values of rill spacing interval. In general, the sediment transport rate and the accumulated erosion amount increase with decreasing rill spacing interval. That is to say, the greater the number of rills in an area, the more sediment transport rate and accumulated erosion amount there are on the hillslope. Because rill erosion is more serious than interrill erosion, it is important to control the generation of rills on the hillslope. In fact, the generation of rills, to a great extent, depends on the slope length, rainfall intensity, soil properties, etc. Among these, the slope length is a major factor for rill generation. In addition, the slope length may obviously affect the rate of soil erosion, as shown before. As a result, controlling the slope length is an effective engineering measure for reducing soil erosion.

CONCLUDING REMARKS

By coupling the kinematic wave model for overland flow, the revised Green–Ampt formula for infiltration, a model for interrill erosion, and a model for rill erosion, an unsteady soil erosion model was developed for hillslopes. The model-simulated results compared satisfactorily with experimental observations. Some basic

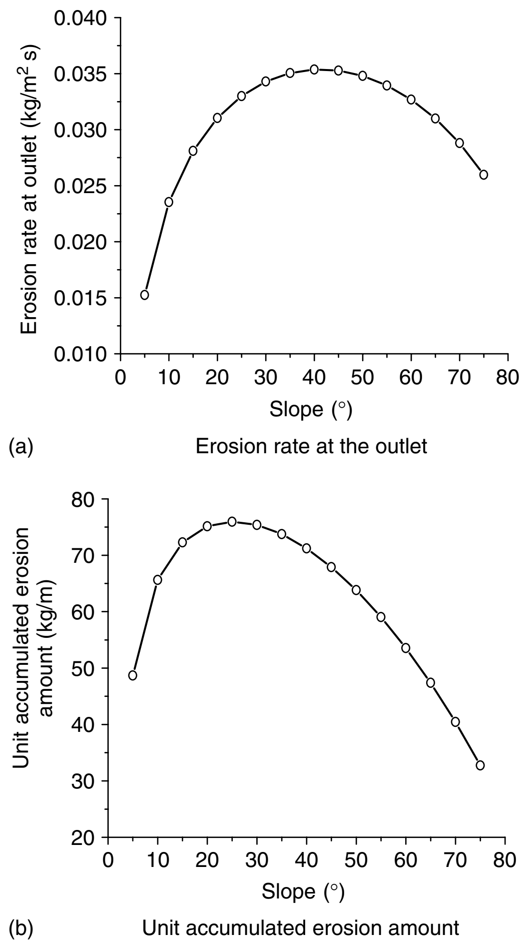

Figure 7. Influence of slope gradient on soil erosion

characteristics of soil erosion on slopes were analysed by simulation. The following conclusions are drawn from this study:

1. Both sediment transport rate and accumulated erosion amount increase remarkably as rainfall intensity increases. However, neither increases linearly with rainfall intensity.
2. The same rainfall amount but with different rainfall processes may cause different erosion results. Although these differences are small, there exists a trend that the later the rainfall peak value is, the higher are the maximum values of the main hydraulic parameters. Similarly, the later the rainfall peak value, the higher the eroding capability, which can lead to more serious soil erosion.
3. The sediment transport rate and cumulative erosion amount increase remarkably as the slope length increases. The sediment transport rate increases nonlinearly along the slope, and soil erosion becomes more serious with the increase of the slope length. The influence of slope length becomes gradually weaker when the slope length decreases to a certain extent. This result reveals that short slopes would be beneficial for decreasing soil erosion.
4. There exists a critical slope gradient for soil erosion. With increasing slope gradient, the soil erosion rate at the outlet and accumulated erosion amount first increase to a peak value, then decrease again. However,

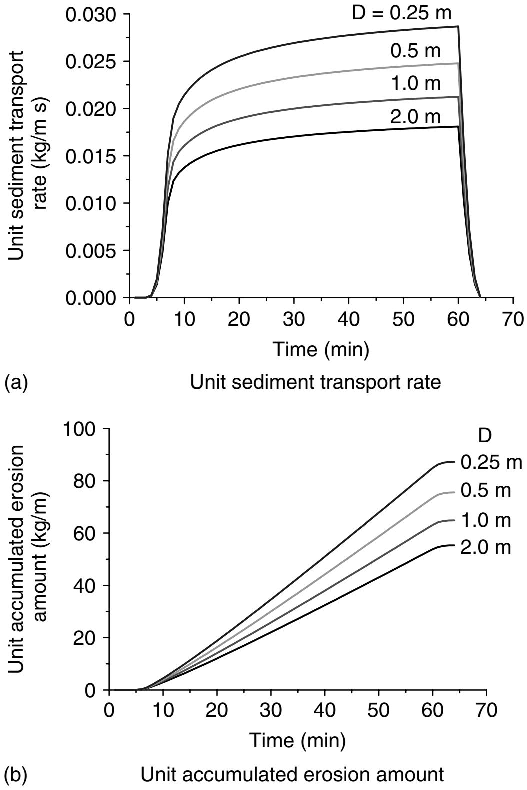

Figure 8. Influence of rill density on soil erosion

the critical slopes are different for erosion rate at the outlet and the total erosion amount. The critical slope gradient is about 45° for erosion rate at the end of the slope, but about 25° for the accumulated erosion amount. This result may be significant for programming the utilization of slope land in the Loess Plateau area of China.

5. Sediment transport rate and total erosion amount increase with the decrease of the rill spacing interval. That is to say, the greater the number of rills in a hillslope area, the more the sediment transport rate and total erosion amount there are on the hillslope. Controlling the generation of rills on a slope is important for reducing soil loss.

ACKNOWLEDGMENTS

This research was financially supported by the National Natural Science Foundation of China (No. 19832060 and No. 10332050).

APPENDIX A: NOTATION

The following symbols are used in this paper:

a	parameter
as	parameter

b	parameter
C	sediment concentration (kg m^{-3})
c_f	the conflux coefficient of overland flow concentrating into rills from interrill areas
d	diameter of sediment (m)
D	the spacing interval between two rills (m)
d'	characteristic diameter (m)
D_i	interrill erosion rate (kg m^{-2} s^{-1})
D_r	rill erosion rate (kg m^{-2} s^{-1})
d_{50}	the median grain size of sediment (m)
d_*	referenced diameter (m)
G	parameter, $G = 0{\cdot}635Y_c^{-1}[1 - \ln(1 + \text{as})/\text{as}]$
g	acceleration due to gravity (m s^{-2})
h	water depth (m)
I	the total infiltration (m)
i	infiltration rate (m s^{-1})
I_p	the cumulative infiltration when the infiltration rate equals rainfall intensity (m)
K	the saturate conductivity of soil (or infiltration coefficient) (m s^{-1})
k	nondimensional parameter, $k = 0{\cdot}128$
L	the length of slope (m)
n	Manning roughness coefficient (s m$^{-1/3}$)
p	Rainfall intensity (m s^{-1})
q	unit discharge of overland flow (m^2 s^{-1})
q_s	sediment transport rate per unit width (kg m^{-1} s^{-1})
R	hydraulic radius (m)
R_c	unit transport capacity of interrill flow (kg m^{-1} s^{-1})
S	soil suction (m)
s	parameter, $s = \sigma_s/\sigma$
S_0	Slope gradient, $S_0 = \sin\theta$
S_f	Energy slope
S_r	source term of sediment equation
t	the coordinates of time (s)
t_p	the time that rainfall begins to pond (s)
T_c	unit transport capacity of rill flow (kg m^{-1} s^{-1})
u	the mean velocity of rill flow (m s^{-1})
W	the width of slope (m)
x	the coordinate along the slope (m)
Y	dimensionless shear stress, $Y = \tau/[(\rho_s - \rho)gd]$
Y_c	dimensionless critical shear stress, $Y_c = \tau_c/[(\rho_s - \rho)gd]$
α	coefficient (m^{-1})
δ	the thickness parameter of the water film (m)
ε_0	the parameter of the adhesion force(m^3 s^{-2})
γ_0	the dry specific weight of soil (N m^{-3})
γ_0*	the stable dry specific weight of soil (N m^{-3})
θ	the slope angle (°)
θ_i	the initial volumetric water content (m^3 m^{-3})
θ_s	the saturate volumetric water content (m^3 m^{-3})
ρ	the density of fluid (kg m^{-3})

ρ_s	the density of sediment (kg m^{-3})
τ	flow shear stress (Pa)
τ_c	Critical shear stress (Pa)

REFERENCES

Ascough II JC, Baffaut C, Nearing MA, Liu BY. 1997. The WEPP watershed model: I. Hydrology and erosion. *Transactions of the ASAE* **40**(4): 921–933.

Beasley DB, Huggins LF, Monke EJ. 1980. ANSWERS: a model for watershed planning. *Transactions of the ASAE* **23**: 938–944.

Bradford JM, Foster GR. 1996. Interrill soil and slope steepness factors. *Soil Science Society of America Journal* **60**: 909–915.

Bulygin SY. 2001. Challenges and approaches for WEPP interrill erodibility measurements in the Ukranie. In *Proceeding of Soil Erosion for the 21st Century International Symposium, Honolulu, Hawaii*. ASAE: St Joseph, MI; 506–509.

Chang SC. 1995. The method of space–time conservation element and solution element—a new approach for solving the Navier Stokes and Euler equations. *Journal of Computational Physics* **119**: 295–324.

Chang SC, Wang XY, Chow CY. 1999. The space–time conservation element and solution element method: a new high-resolution and genuinely multidimensional paradigm for solving conservation laws. *Journal of Computational Physics* **156**: 89–136.

Chen L, Liu QQ. 2001. On the equations of overland flow and one-dimensional equations for open channel flow with lateral inflow. *Mechanics in Engineering* **23**(4): 21–24.

Chen L, Liu QQ, Li JC. 2001. Study on the runoff generation process on the slope with numerical model. *Journal of Sediment Research* **4**: 61–67 (in Chinese).

Chu ST. 1978. Infiltration during an unsteady rain. *Water Resources Research* **14**(3): 461–466.

Cundy TW, Tento SW. 1985. Solution to the kinematic wave approach to overland flow routing with rainfall excess given by the Philip equation. *Water Resources Research* **21**: 1132–1140.

De Roo APJ, Wesseling CG, Ritsema CJ. 1996. LISEM: a single event physically-based hydrologic erosion model for drainage basins I: theory, input and output. *Hydrological Processes* **10**: 1107–1117.

Dou GR. 1999. Incipient motion of coarse and fine sediment. *Journal of Sediment Research* **6**: 1–9 (in Chinese).

Elliot WJ, Laflen JM. 1993. A process-based rill erosion model. *Transactions of the ASAE* **36**(1): 65–72.

Foster GR, Lane LJ, Nearing MA. 1989. Erosion component. In *USDA–Water Erosion Prediction Project, hillslope profile model documentation*. NSERL Report No. 2, US Department of Agriculture, Agricultural Research Service, National Soil Erosion Research Laboratory, West Lafayette, IN; 10.1–10.12.

Gautam MR, Watanabe K, Saegusa H. 2000. Runoff analysis in humid forest catchment with artificial neural network. *Journal of Hydrology* **235**: 117–136.

Govers G. 1987. Initiation of motion in overland flow. *Sedimentology* **34**: 1157–1164.

Grosh JL, Jarrett AR. 1994. Interrill erosion and runoff on various steep slopes. *Transactions of the ASAE* **37**(4): 1127–1133.

Jiang DS. 1997. *Soil and Water Loss in Loess Plateau and the Regulation Mode*. Hydraulic and Water Power Press of China: Beijing.

Li JC, Liu QQ, Zhou JF. 2003. Environmental mechanics in China. *Advances in Applied Mechanics* **39**: 217–306.

Liebenow AM, Elliot WJ, Laflen JM, Kohl KD. 1990. Interrill erodibility: collection and analysis of data from cropland soils. *Transactions of the ASAE* **33**: 1882–1888.

Lighthill MJ, Whitham GB. 1955. On kinematic waves I: flood movement in long rivers. *Proceedings of the Royal Society of London, Series A* **229**: 281–316.

Lisle IG, Rose CW, Hogarth WL, Hairsine PB, Sander GC, Parlange J-Y. 1998. Stochastic sediment transport in soil erosion. *Journal of Hydrology* **204**: 217–230.

Liu QQ, Chen L, Li JC. 2001. Effect of slope gradient on soil erosion. *Applied Mathematics and Mechanics (English Edition)* **22**(5): 510–519.

Liu QQ, Chen L, Li JC, Singh VP. 2004. Two-dimensional kinematic wave model of overland-flow. *Journal of Hydrology* **291**: 28–41.

Low HS. 1989. Effect of sediment density on bed-load transport. *Journal of Hydraulic Engineering, ASCE* **115**: 124–138.

Mein RG, Larson CL. 1973. Modeling infiltration during a steady rain. *Water Resources Research* **9**(2): 384–394.

Moore ID, Burch GJ. 1986. Sediment transport capacity of sheet and rill flow: application of unit stream power theory. *Water Resources Research* **22**: 1350–1360.

Perrone J, Madramootoo CA. 1999. Sediment yield prediction using AGNPS. *Journal of Soil and Water Conservation* **54**(1): 415–419.

Renard KG, Foster GR, Weesies GA, Porter JP. 1991. RUSLE: revised universal soil loss equation. *Journal of Soil and Water Conservation* **46**: 30–33.

Sharma PP, Gupta SC, Foster GR. 1995. Raindrop-induced soil detachment and sediment transport from interrill areas. *Soil Science Society of America Journal* **59**: 727–734.

Singh A, Herrmann A, Kaushal MP. 2001. PAU-REMO: a two dimensional finite element runoff and soil erosion model for agricultural lands. In *Proceeding of Soil Erosion for the 21st Century International Symposium, Honolulu, Hawaii*. ASAE: St Joseph, MI; 334–337.

Singh VP. 1996. *Kinematic Wave Modeling in Water Resources: Surface Water Hydrology*. Wiley: New York.

Singh VP. 1997. *Kinematic Wave Modeling in Water Resources: Environmental Hydrology*. Wiley: New York.

Tang LQ, Chen GX. 1997. The dynamic model of runoff and sediment generation in small watershed. *Journal of Hydrodynamics (Series A)* **12**(2): 164–174 (in Chinese).

Tayfur G. 2001. Modeling two-dimensional erosion process over infiltration surfaces. *Journal of Hydrologic Engineering* **6**(3): 259–262.

Wang WH, Jiao JY. 1996. *Rainfall and Erosion Sediment Yield in Loess Plateau and Sediment Transportation in the Yellow River Basin*. Science Press: Beijing (in Chinese).

Wischmeier WH, Smith DD. 1965. Predicting rainfall-erosion losses from cropland east of the Rocky Mountains. *Agricultural Handbook* No. 282. U.S. Department of Agriculture: Washington DC, USA.
Wischmeier WH, Smith DD. 1978. Predicting rainfall erosion losses. *Agricultural Handbook* No. 537. U.S. Department of Agriculture: Washington DC, USA.
Woolhiser DA. 1975. Simulation of unsteady overland flow. In Unsteady flow in open channels, Mahmood K, Yevjevich V (eds). Water Resources Publications: Fort Collins; 405–508.
Woolhiser DA, Liggett JA. 1967. Unsteady, one dimensional flow over a plane—the rising diagram. *Water Resources Research* **3**(3): 753–771.
Woolhiser DA, Smith RE, Goodrich DC. 1990. *KINEROS, a kinematic runoff and erosion model: documentation and user manual*. ARS-77 USDA-ARS.
Xiang H. 2002. *Studies on the runoff and sediment yield for complex hillslopes*. Masters thesis, Institute of Mechanics, Chinese Academy of Sciences, Beijing.
Yalin MS. 1963. An expression for bed-load transportation. *ASCE, Journal of the Hydraulics Division* **89**: 221–248.
Yang WZ. 1996. On soil moisture in Loess Plateau. In *Soil and Water Conservation in Loess Plateau*, Meng QM (ed.). Yellow River Hydraulic Press: Zhengzhou (in Chinese).
Young RA, Onstad CA, Bosch DD, Anderson WP. 1989. AGNPS: a non-point pollution model for evaluating agricultural watershed. *Journal of Soil and Water Conservation* **44**(2): 164–172.
Zhang KL, Akiyoshi Y, Zhang XQ. 1998. A laboratory study on rill erosion and sediment delivery on the slope. *Geographical Research* **17**(2): 163–170 (in Chinese).
Zhang XC, Nearing MA, Miller WP, Norton LD, West LT. 1998. Modeling interrill sediment delivery. *Soil Science Society of America Journal* **62**(2): 438–444.

